Journal of Biomolecular NMR, **17:** 153–165, 2000.
KLUWER/ESCOM

Interactions of a didomain fragment of the *Drosophila* Sex-lethal protein with single-stranded uridine-rich oligoribonucleotides derived from the *transformer* and *Sex-lethal* messenger RNA precursors: NMR with residue-selective [5-^{2}H]uridine substitutions

Insil Kim[a], Yutaka Muto[a], Satoru Watanabe[a,*], Aya Kitamura[a], Yasuhiro Futamura[a], Shigeyuki Yokoyama[a,**], Kazumi Hosono[b], Gota Kawai[b], Hiroshi Takaku[b], Naoshi Dohmae[c], Koji Takio[c], Hiroshi Sakamoto[d] & Yoshiro Shimura[e]

[a]*Department of Biophysics and Biochemistry, Graduate School of Science, University of Tokyo, 7-3-1 Hongo, Bunkyo-ku, Tokyo 113-0033, Japan;* [b]*Department of Industrial Chemistry, Chiba Institute of Technology, 2-17-1 Tsudanuma, Narashino, Chiba 275-0016, Japan;* [c]*Institute of Physical and Chemical Research (RIKEN), 2-1 Hirosawa, Wako-shi, Saitama 351-0198, Japan;* [d]*Department of Biology, Faculty of Science, Kobe University, 1-1 Rokkodai, Nada-ku, Kobe 657-0013, Japan; and* [e]*Biomolecular Engineering Research Institute, 6-2-3 Furuedai, Suita, Osaka 565-0874, Japan*

Received 15 December 1999; Accepted 18 April 2000

Key words: isotope labeling, residue-selective, resonance assignment, RNA-binding domain, Sex-lethal, single-stranded RNA

Abstract

Proteins that contain two or more copies of the RNA-binding domain [ribonucleoprotein (RNP) domain or RNA recognition motif (RRM)] are considered to be involved in the recognition of single-stranded RNA, but the mechanisms of this recognition are poorly understood at the molecular level. For an NMR analysis of a single-stranded RNA complexed with a multi-RBD protein, residue-selective stable-isotope labeling techniques are necessary, rather than common assignment methods based on the secondary structure of RNA. In the present study, we analyzed the interaction of a *Drosophila* Sex-lethal (Sxl) protein fragment, consisting of two RBDs (RBD1–RBD2), with two distinct target RNAs derived from the *tra* and *Sxl* mRNA precursors with guanosine and adenosine, respectively, in a position near the 5′-terminus of a uridine stretch. First, we prepared a [5-^{2}H]uridine phosphoramidite, and synthesized a series of ^{2}H-labeled RNAs, in which all of the uridine residues except one were replaced by [5-^{2}H]uridine in the target sequence, GU_8C. By observing the H5-H6 TOCSY cross peaks of the series of ^{2}H-labeled RNAs complexed with the Sxl RBD1–RBD2, all of the base H5-H6 proton resonances of the target RNA were unambiguously assigned. Then, the H5-H6 cross peaks of other target RNAs, GU_2GU_8, AU_8, and UAU_8, were assigned by comparison with those of GU_8C. We found that the uridine residue prior to the G or A residue is essential for proper interaction with the protein, and that the interaction is tighter for A than for G. Moreover, the H1′ resonance assignments were achieved from the H5-H6 assignments. The results revealed that all of the protein-bound nucleotide residues, except for only two, are in the unusual C2′-*endo* ribose conformation in the complex.

Introduction

In eukaryotes, the RNA products of gene transcription are subjected to post-transcriptional controls, such as the splicing of mRNA precursors, and the regulation of mRNA stability, localization, and translation. These processes are mediated by a variety of RNA-binding proteins. The RNA-binding domain (RBD), also referred to as a ribonucleoprotein (RNP) domain or an RNA recognition motif (RRM), is the most frequently found module in RNA-binding proteins (for a review, see Burd and Dreyfuss, 1994). The reported tertiary

*Present address: Biophysics Division, Research Institute, National Cancer Center, 5-1-1 Tsukiji, Chuou-ku, Tokyo 104-0045, Japan.
**To whom correspondence should be addressed. E-mail: yokoyama@biochem.s.u-tokyo.ac.jp

structures of RBD·RNA complexes are divided into two types with respect to the target RNAs. One is RNA that forms a secondary structure by intramolecular base pairing, which is essential for the recognition by the RBD, such as U1 snRNP A (U1A) and U2 snRNP B″ (U2B″) RBDs (for a review, see Varani and Nagai, 1998). In these complexes, the single-RBD proteins mainly recognize the single-stranded loop closed by the base pairs of the secondary-structured RNA, as determined by X-ray crystallography and NMR spectroscopy (Oubridge et al., 1994; Allain et al., 1996; Price et al., 1998).

The other type is non-secondary-structured RNA, which may not form any base pairs in the complex. In contrast to secondary-structured RNA, the recognition of single-stranded RNA or DNA by an RBD-containing protein is different between the determined structures of the complexes, such as hnRNP A1·telomeric DNA (Ding et al., 1999), *Drosophila* Sex-lethal·*transformer*-derived polypyrimidine tract (PPT) (Handa et al., 1999), and poly(A)-binding protein·polyadenylate (Deo et al., 1999). All of the determined tertiary structures of the complexes have the common features that these involve two RBDs in tandem, and both of the RBDs collaborate in defining the nucleotide-sequence specificity of the protein. However, with respect to the specific recognition of their cognate RNAs, RBDs use a variety of interaction modes and form different interaction surfaces, such as antiparallel and parallel extended troughs and a V-shape cleft, for their cognate RNAs. There is still the possibility of other recognition modes, due to the amino acid sequence diversity within RBDs and the variety of target RNA sequences.

To determine the tertiary structures of RBD·RNA complexes by NMR, we must overcome some obstacles. The resonance assignments for single-stranded RNA are the most difficult obstacle, and there actually have been no reports of the NMR structure of a protein·single-stranded RNA complex. Although the U1A RBD·RNA complex has been determined by NMR (Allain et al., 1996), the RNA forms the stem/loop secondary structure by intramolecular base pairing, which is very helpful for the resonance assignment of the RNA (Gubser and Varani, 1996). By contrast, for single-stranded RNAs, the residue-selective labeling of RNA is the most powerful and reliable tool to resolve this problem. We reported the utility of residue-selective isotope labeling as applied to the *transformer* (*tra*) pre-mRNA-derived decamer (GU_8C), which is one of the *Drosophila* Sex-lethal (Sxl) target RNAs, by using [3-^{15}N]uridine (Kim et al., 1997). In the present study, by using a [5-^{2}H]uridine phosphoramidite, we unambiguously assigned all of the base protons of the target RNA in a complex with the Sxl RBD1–RBD2, and propose the possibility of determining the solution structure of a single-stranded RNA complexed with a protein by NMR.

Based on the unambiguous resonance assignment of the base protons, we could compare the recognition of the two different target RNAs of Sxl. The Sxl protein plays key roles in the regulation of gene expression, such as the female-specific alternative splicing not only of the *tra* pre-mRNA (Boggs et al., 1987; Sosnowski et al., 1989; Inoue et al., 1990) but also of its own pre-mRNA (Sakamoto et al., 1992) and the dosage compensation (Zhou et al., 1995). However, the exact sequence of the target RNAs recognized by the Sxl RBD1–RBD2 is not clear yet. There is a difference between the expected target sequence in the *Sxl* pre-mRNA and that in the *tra* pre-mRNA. In addition, different target RNA sequences for Sxl binding have been proposed by in vitro selection (Sakashita and Sakamoto, 1994; Singh et al., 1995). Therefore, we compared the interactions of the Sxl RBD1–RBD2 with the 5′-terminal regions of target RNA sequences, based on the *Sxl* and *tra* pre-mRNAs with guanosine and adenosine, respectively.

Materials and methods

[5-^{2}H]Uridine phosphoramidite

The [5-^{2}H]uridine was prepared as previously described (Kim et al., 1995). Hydrogen–deuterium exchange at the 5 position of uridine was performed in the presence of cysteine (Wataya and Hayatsu, 1972). Uridine and cysteine (10 g each) were dissolved in 200 ml of 98% $^{2}H_2O$, and the pH of the solution was adjusted to 8.6 with NaOH tablets. The deuterium incorporation at the C-5 position of uridine proceeded to an extent of about 90% by a 48 h incubation at 65 °C. The conversion of [5-^{2}H]uridine to the [5-^{2}H]uridine phosphoramidite was carried out according to published procedures (Hakimelahi et al., 1981). The 5′ position was protected with a dimethoxytrityl (DMTr) group, and the 2′ position was protected with a *tert*-butyldimethylsilyl (tBDMS) group. Phosphitylation of the 5′,2′-protected [5-^{2}H]uridine was then performed. All building blocks were satisfactorily characterized by ^{1}H- and ^{31}P-NMR.

RNA preparation

RNAs (GU_8C, GU_2GU_8, AU_8, and UAU_8) were synthesized on a DNA/RNA synthesizer (PerSeptive Biosystems) using 1 μmol of protected nucleoside grafted onto a long chain alkylamine CPG support. The final DMTr-group was removed. The deprotection was performed as previously described (Kim et al., 1997). For desalting, a Sep-Pak cartridge (Waters) was used and then the RNA was quantified by UV spectroscopy. RNA oligomers were purified by 20% polyacrylamide gel electrophoresis (PAGE). After PAGE, the purified RNA was eluted with distilled H_2O at 50 °C for 2 days. The purified RNA sample was desalted on a Sep-Pak cartridge, which was washed with 50 mL of 0.1 M TEAA and distilled H_2O, and was then eluted with 40% acetonitrile. The fractions were evaporated and then checked by UV spectroscopy.

Preparation of [$^{13}C/^{15}N$] selectively labeled RNA

A template DNA for in vitro transcription was designed to contain the promoter sequence of the T7 RNA polymerase, the purine-rich element (GGGAGA), and six repeats of the 11-nucleotide sequence (TAT_8G). In addition, it was flanked by the *Pst*I restriction site and the *Eco*RI restriction site on the 5′- and 3′-sides, respectively. The DNA fragment was cloned between the *Pst*I and the *Eco*RI sites of the pUC119 vector. The plasmid was prepared on a large scale (500 μg), and was treated with *Eco*RI for run-off transcription. The T7 RNA polymerase was purified as described by Zawadzki and Gross (1991). The enzyme reaction was performed in 3 ml of 130 mM HEPES-NaOH buffer (pH 8.1) containing 16 mM $MgCl_2$, 40 mM KCl, 2 mM spermidine, 4 mM ATP, 4 mM GTP, 4 mM CTP, 4 mM [$^{13}C/^{15}N$] UTP, and 150 μg linearized plasmid DNA. After transcription, the transcribed RNA was extracted by phenol/chloroform (1:1) treatment. After the addition of 2.5 M ammonium citrate and 50% 2-propanol, the transcript was precipitated by centrifugation at 10 000 × *g* for 12 min, and the supernatant was removed. The yield of RNA was as high as 50 A_{260} units per ml reaction volume. The 2-propanol precipitation was much more efficient than the ethanol precipitation for the elimination of NTPs. Without any further purification, therefore, we could proceed to the ribonuclease (RNase T1) treatment. The RNA transcript was dissolved in 50 mM Tris-Cl buffer (pH 7.5) containing 1 mM EDTA and 0.01% Triton X-100, to which RNase T_1 (Pharmacia) was added. Digestion was performed overnight at 37 °C. Thus, the RNA transcript was cleaved at all of the guanosine sites by RNase T_1, resulting in the major product, UAU_8G. Purification of the RNA(UAU_8G) was performed by electrophoresis on a 20% polyacrylamide gel containing 7 M urea and 10% glycerol. The RNA in the gel was eluted with distilled H_2O at 50 °C for 2 days and was desalted as described above.

Preparation of the RNA-binding domain fragment (RBD1–RBD2) of the Sxl protein

The gene encoding the RBD1–RBD2 region of the Sxl protein was cloned by PCR methods, and four site-directed mutations, Phe166→Tyr (Inoue et al., 1997; Kim et al., 1997), Tyr142→His, Arg146→Ser, and Ala147→Arg, were introduced into the didomain fragment, the Sxl RBD1–RBD2. *Escherichia coli* strain BL21(DE3), transformed with a T7 RNA polymerase expression vector containing the gene for the mutant RBD1–RBD2 fragment (pK7-RBD1–RBD2), was pre-cultured in 20 mL LB medium to the stationary phase. This pre-culture was added to 1 L of the culture medium, and the cells were cultured, induced with IPTG, and harvested; 4 g of wet cells were collected from 1 L of 2 × M9 medium with 1 g/L NH_4Cl, 240 mg/L $MgSO_4$, 15 mg/L $CaCl_2$, 20 mg/L thiamine, and 4 g/L glucose. Chromatographic purification of the mutant RBD1–RBD2 protein was performed on DEAE Sephacel, CM-Toyopearl, and FPLC Mono S columns. About 10–20 mg of RBD1–RBD2 was obtained from the 4 g of wet cells. Yields of the RBD1–RBD2 protein were estimated by specific absorbance, A280 = 0.56 cm/1 mg × 1 mL.

Preparation of NMR samples

For NMR measurements, 4 mg of the Sxl RBD1–RBD2 in 100 mM potassium phosphate buffer (pH 6.5) was concentrated by ultrafiltration using either Centricon-3 or Centriprep-3 units (Amicon). To prepare the sample of the RNA·protein complex, 1 mM DTT and 20 units of RNase inhibitor (Toyobo) were added to the protein solution. Then, the protein solution was added to the evaporated RNA samples. The samples were washed 2 or 3 times with 99.85% ^2H_2O (Isotec Inc.) containing 100 mM acetic acid-d_4 and 1 mM DL-1,4-DTT-d_{10} by Centricon-3 ultrafiltration. The final samples used for NMR measurements were 0.18-mL solutions containing 1 mM protein and 1 mM RNA.

NMR spectroscopy

All NMR spectra were measured with a Bruker DRX-600 spectrometer, and were processed and analyzed using the UXNMR program (Bruker, Karlsruhe). All of the spectra were acquired at a probe temperature of 298 K. The 2D NOESY spectra were taken with a data matrix consisting of 512 ($t1$) × 2048 ($t2$) complex data points. The spectral widths were 7002 Hz in both dimensions, and a total of 96 scans per $t1$ increment were collected. Solvent suppression was achieved by presaturation and with an NOE mixing time of 150 or 250 ms. In the 2D TOCSY spectra, the data matrices consisted of 512 ($t1$) × 2048 ($t2$) complex data points. A total of 96 scans per $t1$ increment were collected, and the spectral widths were 7002 Hz in both dimensions. For the isotropic mixing, an MLEV17 pulse train of 45 ms was used. A two-dimensional (2D) ^{1}H–^{13}C HSQC spectrum was acquired (Bax et al., 1990). Quadrature detection was achieved using the States-TPPI method. All data were zero-filled to 4096 × 2048 complex data points, and were apodized with a squared sine-bell function in both dimensions.

Results and discussion

Improvement of the solubility of the Sxl RBD1–RBD2 by mutagenesis

We have increased the solubility of the Sxl RBD1–RBD2, without affecting the RNA-binding properties, through the mutation of Phe166 to Tyr (Inoue et al., 1997; Kim et al., 1997). Nevertheless, the Phe166→Tyr mutant RBD1–RBD2 exhibited aggregation to some extent. Therefore, in the present study, we tried to improve the Sxl RBD1–RBD2 solubility further by additional mutations, modeled after the U1A RBD mutant that exhibits increased solubility of the RNA·protein complex with the same RNA-binding ability as the wild type (Oubridge et al., 1994; Howe et al., 1998). Thus, three mutations, Tyr142→His, Arg146→Ser, and Ala147→Arg, were introduced to the Phe166→Tyr mutant of the Sxl RBD1–RBD2. These additional mutation sites are exposed on an α-helix situated on the side opposite the putative RNA-interacting surface of the Sxl RBD1 β-sheet. The quadruple mutant RBD1–RBD2 was shown to bind the Sxl-binding, *tra*-derived decamer (5′GUUUUUUUUC3′ or GU_8C) (Kanaar et al., 1995) as well as the wild-type RBD1–RBD2 and the previously constructed, single mutant; these three proteins exhibited the imino proton resonances of the bound RNA at the same chemical shifts (data not shown). Furthermore, the present mutant didomain fragment actually exhibited much higher solubility and stability of the RNA complex than the previous mutant, as judged from the degree of aggregation at high concentrations.

Sequential NOEs of the RNA

We examined the interaction of the highly soluble mutant of the Sxl RBD1–RBD2 with GU_8C. In the aromatic region of the TOCSY spectrum of the RNA·protein complex (Figure 1a), eight strong and one weak H5-H6 cross peaks of the pyrimidine moieties were observed. In the absence of the Sxl RBD1–RBD2, the resonances originating from the uridine residues in GU_8C were heavily overlapped in a very narrow region (data not shown). In contrast, when the RNA was complexed with the Sxl RBD1–RBD2, the resonances of these repetitive uridine residues were dispersed well in the NOESY and the TOCSY spectra (Figure 1). Nine H5-H6 cross peaks, which originated from all of the pyrimidine residues, were identified in the TOCSY spectrum. This indicates that the local environments around these uridine residues became different from each other upon complex formation. With the aid of these H5-H6 cross peaks of the TOCSY spectrum, we tried to elucidate the sequential connectivities between the base proton resonances on the basis of the NOESY cross peaks. In canonical A-form RNA, the sequential H1′(i)-H6/H8($i+1$) distance and the intra-residue H1′(i)-H6/H8(i) distance are about 3.5–4.5 Å. Therefore, each aromatic resonance shows two weak or moderate NOESY cross peaks in the aromatic/anomeric region, which is a pivotal basis for the sequence-specific resonance assignments of structurally ordered RNAs (Varani et al., 1996). Actually, in the structure of the complex between the U1A RBD and PIE RNA with a seven-nucleotide internal loop (Allain et al., 1996), which is the only RBD·RNA complex structure determined by NMR methods thus far, the A-form base stacking extends from the stem to the first three bases of the loop, and the last two bases of the loop are also stacked on each other. These features made it possible to assign the homonuclear NOESY cross peaks of the RNA in the complex (Gubser and Varani, 1996).

To try a similar manner of resonance assignment, we obtained the NOESY spectra of the GU_8C·protein complex at various mixing times, including a 250-ms mixing time (Figure 1b). However, when we tried to

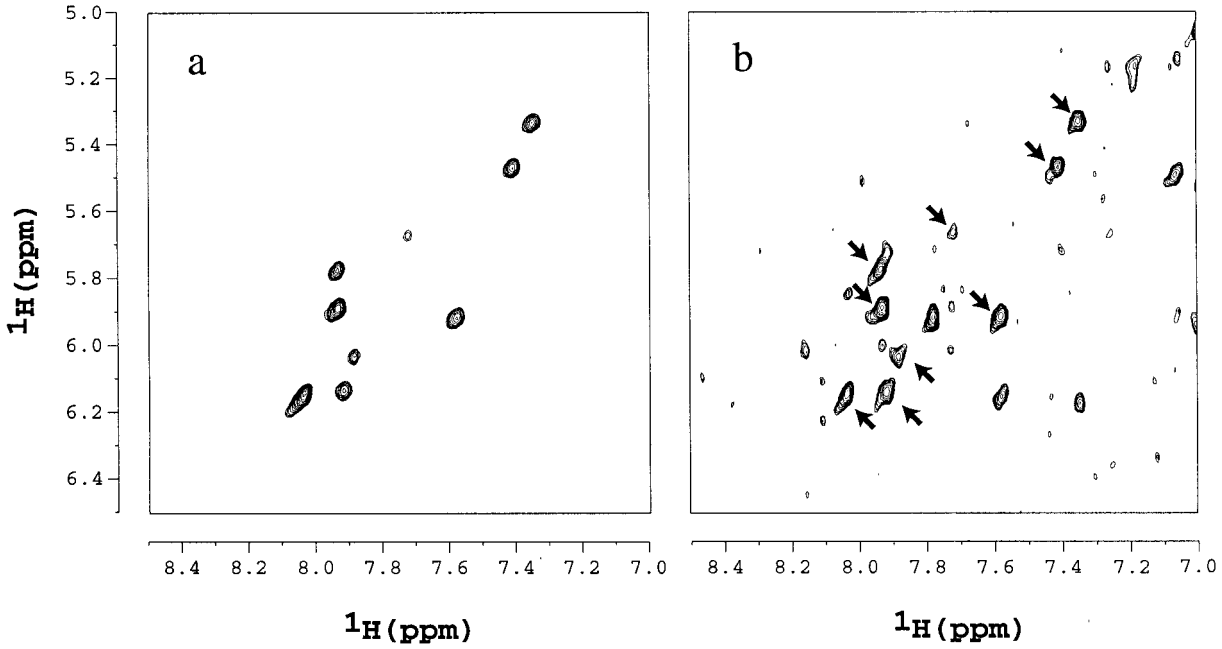

Figure 1. The aromatic regions of the TOCSY spectrum (a) and the NOESY spectrum (mixing time 250 ms) (b) of the Sxl RBD1–RBD2·GU_8C complex in ^2H_2O at 298 K. Nine H5-H6 cross peaks, one of which is weak, are observed not only in (a) but also in (b), as indicated with arrows.

trace the sequential NOEs in the aromatic/anomeric region, only a few base moieties exhibited sequential NOEs, and the rest showed only one weak NOE each to the H1′ proton (Figure 1b). This result indicates that the conformation of GU_8C complexed with the Sxl RBD1–RBD2 in solution is quite different from the canonical A-form RNA, and is consistent with the crystal structure of the Sxl RBD1–RBD2·*tra* polyuridine tract complex with mostly unstacked base moieties. Thus, the resonance assignments based on the sequential NOEs were not successful in this complex.

Full resonance assignment of the RNA base protons

For NMR analyses of RNA, the usefulness of residue-selective [5-^{2}H]uridine substitution has been pointed out from two aspects: the unambiguous resonance assignments (Kim et al., 1995) and the 'NMR-window' concept (Földesi et al., 1996). In the present study, we applied this method to a large RNA·protein complex for the first time, to achieve unambiguous resonance assignments. For the chemical synthesis of labeled RNAs, [5-^{2}H]uridine was prepared and converted to [5-^{2}H]uridine phosphoramidite. Then, we synthesized a series of ^{2}H-labeled GU_8C samples in which all of the uridine residues, except one, were replaced by [5-^{2}H]uridine. For example, in the U2-selectively ^{2}H-unlabeled RNA, seven uridine residues, U1 and U3-U8, were replaced by [5-^{2}H]uridines, while U2 remained unlabeled ([5-^{1}H]uridine). In the TOCSY spectra of this RNA, the U2 resonances could easily be distinguished from the other uridine resonances, since the H5-H6 cross peak was fully observed only for the U2 residue.

Figure 2 shows the H6 and H1′/H5 region of the TOCSY spectra of the U2-selectively ^{2}H-unlabeled RNA (Figure 2a) and the U6-selectively ^{2}H-unlabeled RNA (Figure 2b), in the Sxl RBD1–RBD2-bound state. In the present experiments, the incorporation of ^{2}H at position 5 of the uridine base was about 90%. As compared with Figure 1a, six out of the nine H5-H6 cross peaks were not observed at a higher threshold level (Figure 2a), and could be observed only at a lower threshold level (Figure 2c). On the other hand, three H5-H6 cross peaks were clearly observed in Figure 2a. Among these three strong H5-H6 cross peaks, two cross peaks at 5.89/7.93 and 6.15/8.02 ppm were also observed for the U6-selectively ^{2}H-unlabeled RNA (Figure 2b) and all of the other residue-selectively ^{2}H-unlabeled RNAs in the protein-bound state (they were assigned to those of U8 and the 3′-terminal C, as described below). Therefore, we assigned the remaining peaks, observed at 5.33/7.33 ppm, to the H5-H6 cross peak of U2 (Figure 2a). Similarly, the U6-selectively ^{2}H-unlabeled

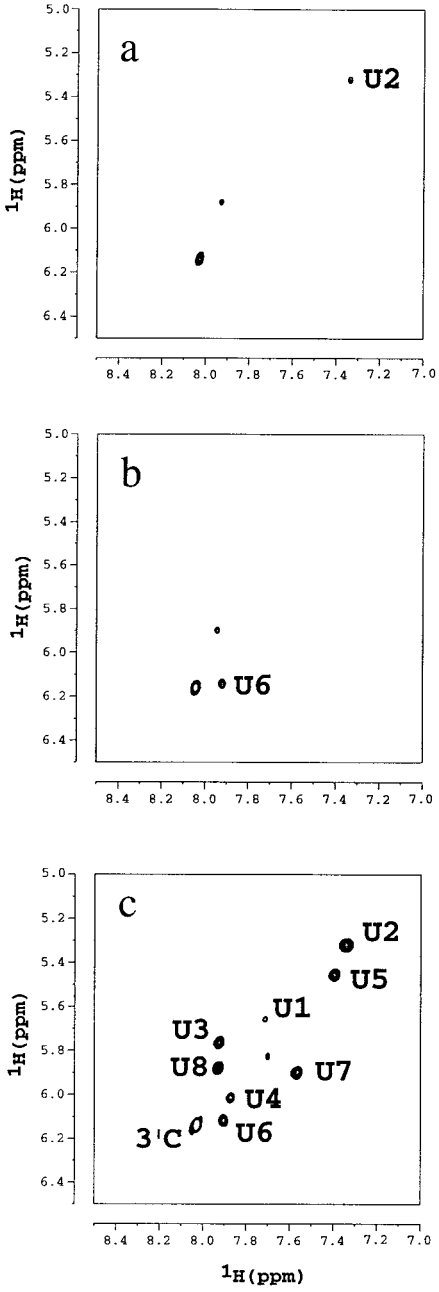

Figure 2. Comparison of the aromatic regions (H6 and H5) of the TOCSY spectra between the U2-selectively ^{2}H-unlabeled RNA (GUUUUUUUUC) (a) and the U6-selectively ^{2}H-unlabeled RNA (GUUUUUUUUC) (b), where U is 5-^{2}H-labeled and U is unlabeled, as complexed with the Sxl RBD1–RBD2. The H5-H6 cross peaks due to U2 and U6 are observed only in (a) and (b), respectively, while the sharp H5-H6 cross peak of the residual [5-^{1}H]U8 and that of the unlabeled 3′-terminal C are observed in both (a) and (b). The TOCSY spectrum of the U2-selectively ^{2}H-unlabeled RNA at an eightfold lower threshold level (c) shows all of the weak cross peaks due to the residual [5-^{1}H]uridines at the other ^{2}H-labeled positions. The assignments of the H5-H6 cross peaks are shown in (c).

RNA·Sxl protein complex exhibited three H5-H6 cross peaks at 5.89/7.93, 6.15/8.02, and 6.14/7.90 ppm in the TOCSY spectrum, and the H5-H6 cross peak at 6.14/7.90 ppm was assigned to that of U6 (Figure 2b). In this manner, by using the seven ^{2}H-labeled RNAs, we unambiguously assigned all of the H5-H6 resonances of U1, U2, U3, U4, U5, U6, and U7.

Consequently, the other two H5-H6 cross peaks, which were well observed at 5.89/7.93 and 6.15/8.02 ppm in all of the TOCSY spectra, must be assigned to the residual [5-^{1}H]uridine at position U8 and the 3′-terminal cytidine, which follows U8. The 6.15/8.02 ppm cross peak is much stronger than the 5.89/7.93 ppm cross peak and the uridine H5-H6 cross peaks assigned above. The 6.15/8.02 ppm cross peak intensities in the [5-^{2}H]uridine-labeled spectra are the same as that in the spectrum of the normal, fully unlabeled RNA in the protein-bound state (Figure 1a). Therefore, the 6.15/8.02 ppm cross peak is due to the 3′-terminal cytidine. In contrast, the 5.89/7.93 ppm cross peak was observed much less strongly in the TOCSY spectrum of the '[5-^{2}H]U8' RNAs than in that of the normal, fully unlabeled RNA in the complex (Figure 1a). Therefore, the 5.89/7.93 ppm cross peak was assigned to the residual [5-^{2}H]U8, due to the incomplete ^{2}H incorporation into the uracil base. The two cross peaks of U8 and the 3′-C are sharper and stronger than the other H5-H6 cross peaks, indicating that these two nucleotide residues are not in direct contact with the protein. This is the reason why U8 exhibited a rather stronger residual H5-H6 cross peak than the other uridine residues for the [5-^{2}H]uridine-incorporated RNAs. The flexibility of the base moieties of U8 and 3′-C, probably due to the lack of direct contact with the protein, is consistent with the crystal structure, in which the base moiety of the last uridine residue of the protein-bound GUUGUUUUUUUU, which corresponds to the present U8 residue of GUUUUUUUUC, is disordered (Handa et al., 1999). Thus, all of the nine H5-H6 cross peaks were unambiguously assigned, with the series of residue-selectively [5-^{2}H]uridine-substituted RNAs, for the complex of GU_8C and the Sxl RBD1–RBD2 (Figure 2c).

Several methods for the resonance assignment of RNA on the basis of through-bond coherence transfer have been reported (for reviews, see Varani et al., 1996; Wijmenga and van Buuren, 1998). However, in the case of the RNA complexed with the Sxl RBD1–RBD2, the through-bond coherence transfer experiments with a uniformly ^{13}C-labeled RNA were unsuc-

cessful (data not shown), probably because the molecular mass of the present complex is 22 kDa. Similarly, for example, it was reported that triple resonance experiments were unsuccessful for the L30·mRNA complex, whose molecular mass is 22 kDa; several variant RNAs designed on the basis of the biochemical data were used for the unambiguous resonance assignment (Mao and Williamson, 1999). For many RBD-containing proteins, the tandem arrangement of two (or more) RBDs is supposed to be important for specific binding to single-stranded RNAs, and the large molecular mass of the complex of RNA with the didomain (or multidomain) fragment makes it difficult to achieve the resonance assignment by experiments such as through-bond coherence transfer. In these cases, therefore, the present residue-selective isotope labeling would be quite useful for the unambiguous resonance assignments.

Interaction of GU_2GU_8 with the Sxl RBD1–RBD2

On the basis of the unambiguous H5 and H6 resonance assignments of GU_8C bound with the Sxl RBD1–RBD2, we could compare this RNA and GU_2GU_8, which are both derived from the polyuridine tract of the *tra* pre-mRNA. It has been reported that the Sxl RBD1–RBD2 binds to GU_8C with an affinity similar to that for a longer *tra* pre-mRNA (Kanaar et al., 1995). On the other hand, in the crystal structure of the Sxl RBD1–RBD2·GU_2GU_8 complex, the UGU_7 region is bound with the protein, and the uridine residue just prior to the guanosine residue is recognized by Sxl Arg252 (Handa et al., 1999). It has also been reported that the replacement of Arg252 by Ala abolished the ability of the Sxl RBD1–RBD2 to bind to the *tra* polyuridine tract (Lee et al., 1997).

Thus, we compared the NOESY spectra of GU_8C and GU_2GU_8 complexed with the Sxl RBD1–RBD, in order to examine how the interaction of the guanosine residue with the protein is affected by the uridine residue on the 5′ side (Figure 3a,b). In the GU_2GU_8 complex spectrum, the H5 and H6 resonances, corresponding to those of the six uridine residues from U2 to U7 of GU_8C, were observed at the same chemical shifts, respectively. Therefore, the Sxl protein binds to the RNA chain spanning from U2 to U7 of these two RNAs in the same manner. The 5′-GU region (GUUGUUUUUUUU) does not appear to interact with the protein, as their resonances are very sharp and do not exhibit any intermolecular NOEs. The H5 and H6 resonances of U8 in the GU_8C complex are slightly shifted in the GU_2GU_8 complex, because of the deletion of the 3′-C. In contrast, the H5-H6 NOE cross peak of U1 in the GU_8C complex is much weaker than those of the six protein-interacting uridine residues, U2–U7 (Figure 3a), while the corresponding cross peak in the GU_2GU_8 complex is as strong as those of the other protein-interacting uridine residues (Figure 3b). Consequently, the UGU moiety of GU_2GU_8 is tightly bound on the protein, whereas the GU moiety of GU_8C seems to be rather loosely bound. It might be possible that the GU moiety of GU_8C undergoes a rather slow transition between the observed 'major' state and some 'minor' state (at an intermediate rate of exchange on the NMR time scale).

Interactions of UAU_8 and AU_8 with the Sxl RBD1–RBD2

The Sxl protein is known to bind to its own *Sxl* pre-mRNA for autoregulation, in addition to the downstream *tra* pre-mRNA. The *tra* pre-RNA has a single Sxl-binding site with a guanosine residue followed by the polyuridine tract. In contrast, the *Sxl* pre-mRNA has many Sxl-binding polyuridine sequences that contain an adenosine residue (Sakamoto et al., 1992). Actually, our previous studies by residue-selective [3-^{15}N]uridine incorporation revealed that the Sxl RBD1–RBD2 binds AU_8C more tightly than GU_8C and U_8C (Kim et al., 1997). On the other hand, the crystal structure of the Sxl RBD1–RBD2·GU_2GU_8 complex revealed that the characteristic 2-amino group of the second guanosine residue is involved in the interaction with the protein (Handa et al., 1999), which cannot explain how Sxl recognizes the adenosine residue, which lacks the 2-amino group, in the Sxl pre-mRNA sequences. Thus, we compared the NOESY spectra of the two different target RNAs, GU_2GU_8 and UAU_8, complexed with the Sxl RBD1–RBD2 (Figure 3b,d). With the exception of the H5 and H6 resonances of U1, each of those of the U_8 region was observed at the same chemical shift between the two RNA·protein complexes. The difference in the chemical shifts of the H5 and H6 resonances of U1 is due to the effect of the different purines. Therefore, the Sxl protein interacts with most of the U_8 regions in the same manner in the complexes with GU_2GU_8 and UAU_8, while the difference in the purine residue, G and A, respectively, just prior to the uridine stretch may cause some difference in the interaction of U1 with the protein.

Next, we examined the effect of the extra uridine residue prior to the purine residue on the RNA·protein interaction, by measuring the NOESY spectrum of

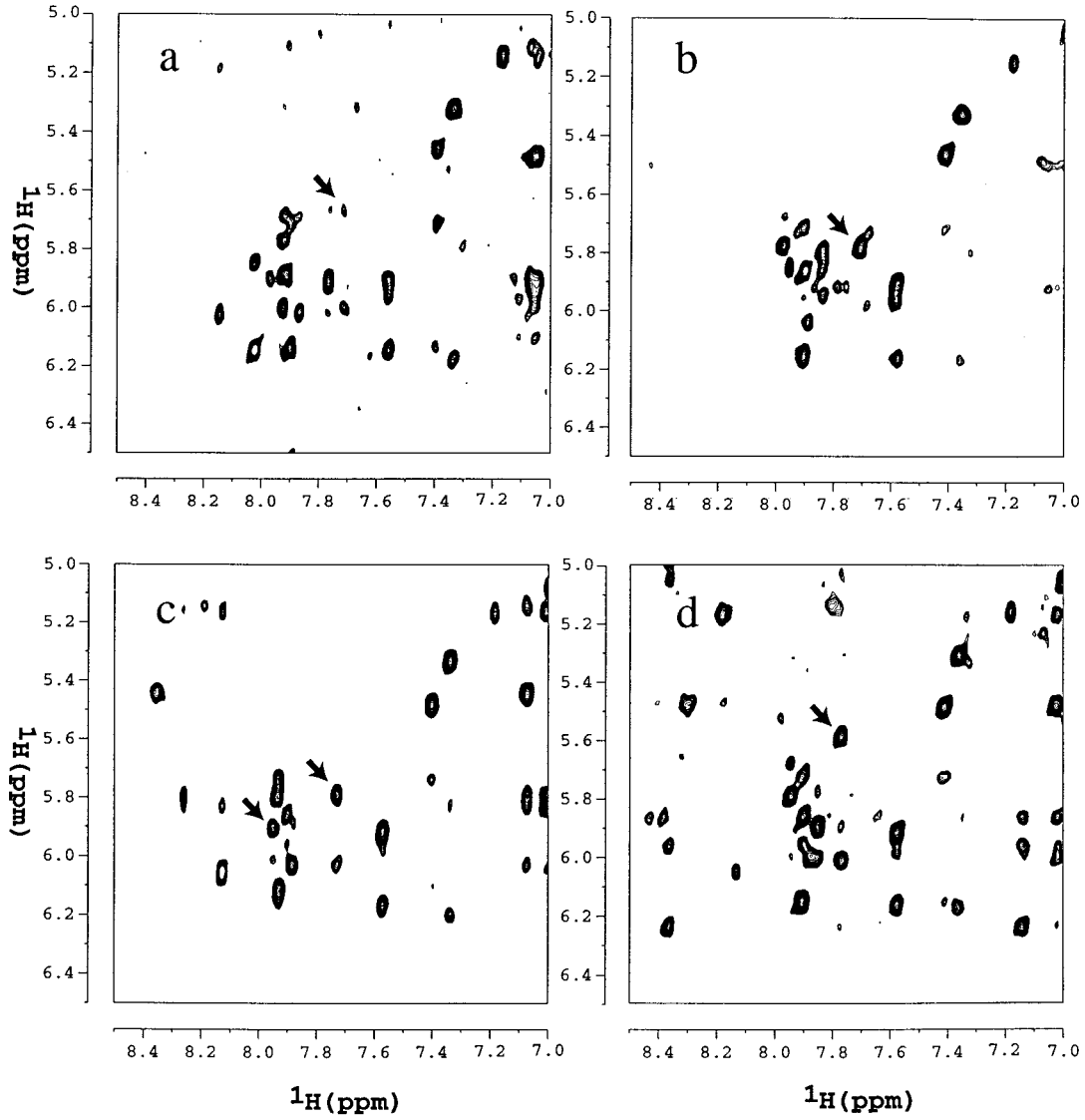

Figure 3. Comparison of the aromatic/anomeric regions in the NOESY spectra of GU_8C (a), GU_2GU_8 (b), AU_8 (c), and UAU_8 (d), as complexed with the Sxl RBD1–RBD2. The H5-H6 cross peaks of U1 are indicated with arrows.

the complex of AU_8 with the Sxl RBD1–RBD2 (Figure 3c). The first uridine residue (U1) of the U_8 region in the AU_8 complex exhibited a set of two H5-H6 cross peaks (Figure 3c), suggesting a slow exchange on the NMR time scale between the two states, which might correspond to the major and minor states suggested above for the GU_8C complex. The number of intermolecular NOEs is appreciably smaller in the AU_8 complex than in the UAU_8 complex. Therefore, the extra uridine residue just prior to the adenosine residue plays an essential role to fix the AU moiety properly on the protein. As judged from the intermolecular NOEs, Sxl RBD1–RBD2 interacts more strongly with A than with G. This result is consistent with our previous observation (Kim et al., 1997).

$^{13}C/^{15}N$ labeled RNA complexed with the Sxl RBD1–RBD2

In vitro transcription using T7 RNA polymerase is the most common method for the preparation of $^{13}C/^{15}N$-labeled RNA (Puglisi and Wyatt, 1995). However, the efficiency of the transcription is very low when the RNA fragment is short and lacks a purine-rich sequence at its 5′ region. The elegant method utiliz-

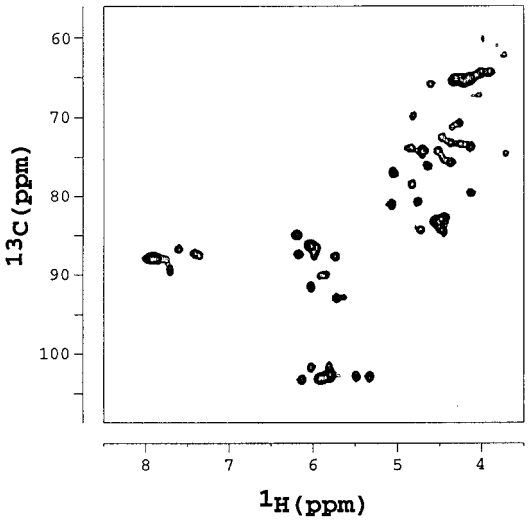

Figure 4. ^{1}H–^{13}C HSQC spectra of [$^{13}C/^{15}N$]-U selectively labeled RNA complexed with the unlabeled Sxl RBD1–RBD2. The C6 resonances were aliased in the F_1 dimension.

ing a ribozyme system has been reported to overcome the low efficiency of transcription (Price et al., 1995). However, to apply this method, it is essential that the transcribed RNA is properly folded to make the ribozyme structure, and this does not always occur in all RNAs. Actually, the application of this method to the target RNA of the Sxl RBD1–RBD2 was not successful (data not shown). In contrast to the *cis*-acting ribozymes, ribonuclease (RNase) T_1 is a *trans*-acting enzyme that cleaves the RNA fragment at the guanosine site. We noted that no guanosine residue was found in the target RNA (UAU_8) of the Sxl RBD1–RBD2. In the present study, the DNA template was designed to generate a long RNA containing 6 repeats of an 11-nucleotide sequence (UAU_8G). By the RNase T_1 treatment, the transcribed RNA was cleaved at all of the guanosine sites and as a result, the desired RNA (UAU_8G) was liberated as the main product. The relative molecular mass of the purified RNA was verified by MALDI-TOF mass spectrometry (data not shown). Therefore, using this method, we obtained as much as 200 μmol of the RNA (UAU_8G) in a 3 ml reaction volume, which was enough for one NMR sample.

Using this [$^{13}C/^{15}N$] selectively labeled RNA, we measured the ^{1}H-^{13}C HSQC spectrum (Figure 4). The chemical shifts of the base protons in this spectrum are the same as those in the homonuclear TOCSY spectrum. Moreover, we could easily identify the H1′ resonances in the ^{1}H-^{13}C HSQC spectrum (Figure 4) and this encouraged us to obtain further resonance assignments. A well-resolved ^{1}H-^{13}C NOESY–HSQC spectrum of the protein·RNA complex was obtained, which showed results consistent with those obtained from the homonuclear NOESY and TOCSY spectra (data not shown).

H1′ resonance assignment

With the sequence-specific resonance assignments of the H5 and H6 resonances established, we next proceeded to the H1′ resonance assignments on the basis of the intra-residue H6-H1′ NOEs. Figures 5a and 5b show the H6-H5/H1′ region of the NOESY spectrum and the H1′-H2′ region of the TOCSY spectrum, respectively, of UAU_8 complexed with the Sxl RBD1–RBD2. Based on the H6 chemical shifts according to the H5-H6 assignments, the H6-H1′ cross peaks were picked up in the NOESY spectrum (Figure 5a), and were then connected to the corresponding H1′-H2′ cross peaks in the TOCSY spectrum (Figure 5b). In addition, we obtained the ^{1}H-^{13}C HSQC spectrum (Figure 4) and the ^{1}H-^{13}C NOESY–HSQC spectrum (data not shown), which were helpful for the assignments.

First, the H6-H1′ and H1′-H2′ cross peaks at 7.85/6.01 and 6.01/4.48 ppm, observed for the UAU_8 complex (Figure 5), were also observed for the GU_2GU_8 complex, but not for either of the AU_8 and GU_8C complexes (data not shown). Therefore, these H1′, H2′, and H6 resonances were assigned to the 5′-terminal uridine residue (5′-U). The H6 resonance of U1 at 7.77 ppm was connected to an H1′ resonance that happened to resonate at the same chemical shift as that of 5′-U. Then, the H1′-H2′ cross peak at 6.01/4.38 ppm, which could be distinguished from that of 5′-U, was assigned to U1. The H6 resonance of U2 was connected to one H1′ resonance at 6.17 ppm, and then to the H2′ resonance at 4.27 ppm.

For U3, the H6-H1′ cross peak was observed at 7.94/5.68 ppm, but the corresponding H1′-H2′ TOCSY cross peak was not observed. The H6-H1′ cross peak of U4 was considered to be overlapped with the H5-H6 cross peak at 7.88/6.02 ppm, and the H1′-H2′ cross peak was again missing in the TOCSY spectrum. These tentative assignments of the H1′ resonances of U3 and U4 were actually confirmed by using the $^{13}C/^{15}N$-labeled RNA (Figure 4). These characteristic properties of U3 and U4 are due to the ribose puckering conformations different from those of other nucleotide residues, as described below.

On the other hand, the H6 resonance of U5 at 7.41 ppm was successfully connected to one H1′

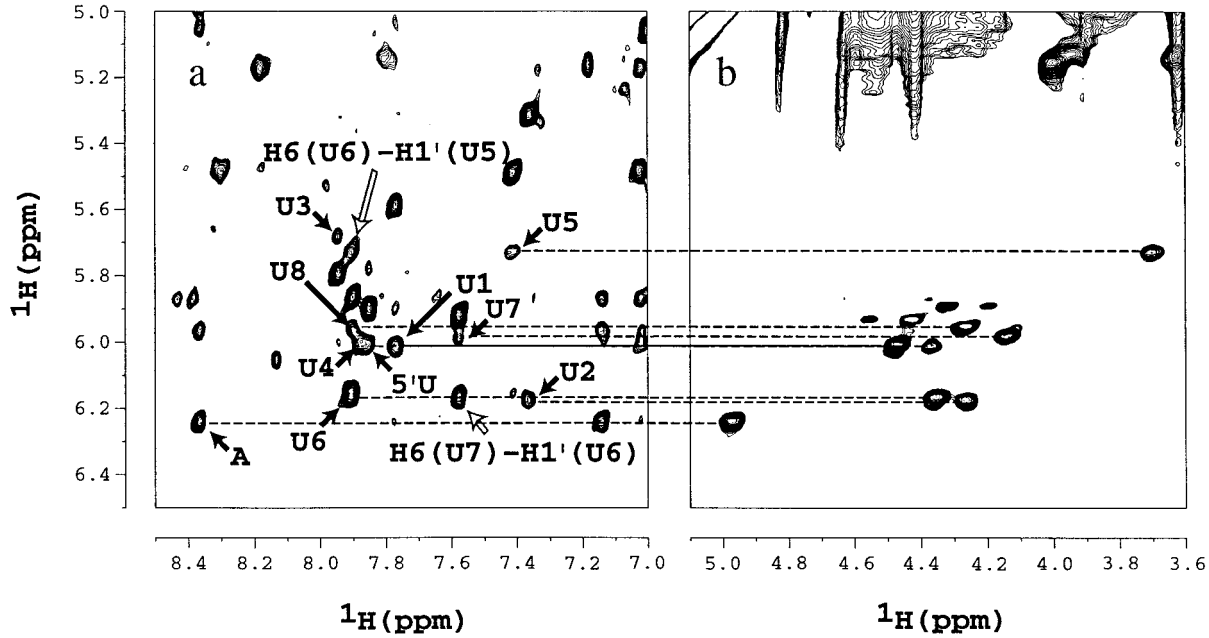

Figure 5. The H1′ proton resonance assignments of UAU_8 complexed with the Sxl RBD1–RBD2. The aromatic/anomeric regions of the NOESY spectrum at 250 ms (a) and the H1′/H2′ region of the TOCSY spectrum (b). The dashed lines show the same chemical shift of H1′ in both spectra. The cross peaks labeled with the filled arrows indicate the intra-nucleotide NOEs between the base H8/H6 proton and the sugar H1′ proton, and those labeled with the open arrows indicate the sequential H6(*i*)-H1′($i-1$) NOEs.

resonance at 5.73 ppm, and then to the H2′ resonance at 3.70 ppm. Next, the H6 resonance of U6 at 7.90 ppm exhibited a sequential H6(*i*)-H1′($i-1$) NOE to the H1′(U5) proton resonating at 5.73 ppm, and an intra-residue NOE to one H1′ proton resonating at 6.16 ppm. Similarly, the H6(U7) resonance at 7.57 ppm was connected to the H1′(U6) proton (6.16 ppm) through the sequential H6(*i*)-H1′($i-1$) NOE, and also to the H1′ resonance at 5.99 ppm through the intra-residue NOE. Concerning the assignments of two sequential NOEs, H6(U6)-H1′(U5) and H6(U7)-H1′(U6), we carefully examined the NOESY, TOCSY, ^{1}H-^{13}C HSQC, and ^{1}H-^{13}C NOESY–HSQC spectra. Except for the assignment described above, we were confronted with inconsistencies in the other assignments. For example, the H1′-H2′ TOCSY cross peak was observed at 6.16/4.34 ppm, and therefore, one of the H1′ protons was resonating at 6.16 ppm. Moreover, in the ^{1}H-^{13}C HSQC spectra, we could identify the H1′ proton resonating at 6.16 ppm, which overlapped with the resonance of H5(U6) in the proton spectra. If we assigned it to H1′(U7), and not to H1′(U6), then the cross peak at 7.57/6.16 ppm would be assigned to the intra-residue NOE between H6(U7) and H1′(U7). Then, the H1′ proton resonating at 5.99 ppm remained to be assigned with no candidate, even though we could identify the intra-molecular TOCSY cross peak between H1′ and H2′ at 5.99 ppm/4.15 ppm. In addition, in the ^{1}H-^{13}C NOESY–HSQC spectra, we observed the NOEs of H6(U6)-H1′(U6) and H6(U7)-H1′(U6) at the F2(^{13}C) chemical shift of 87.36 ppm, corresponding to C1′(U6). Therefore, the above assignments were confirmed. Note that the sequential H6(*i*)-H1′($i-1$) NOEs were exceptionally detectable for U6 and U7. This observation is consistent with the crystal structure of the Sxl RBD1–RBD2·GU_2GU_8 complex, where the H6(*i*)-H1′($i-1$) distances of U6-U5 and U7-U6 are much shorter than those of the other positions of GU_2GU_8 and those in canonical A-form RNA. Then, U8 was found to exhibit the H6-H1′ and H1′-H2′ cross peak pairs at 7.90/5.95/4.26 ppm. Thus, all of the H1′ resonances of 5′-U and the uridine stretch from U1 to U8 were unambiguously assigned. Finally, a strong TOCSY cross peak at 6.24/4.98 ppm was NOE-connected to one resonance at 8.36 ppm, and these three resonances were tentatively assigned to the H1′, H2′, and H8 protons of the single adenosine residue of the RNA. These tentative resonances assignments of the adenosine were actually confirmed by using the ^{13}C/^{15}N-labeled RNA (data not shown).

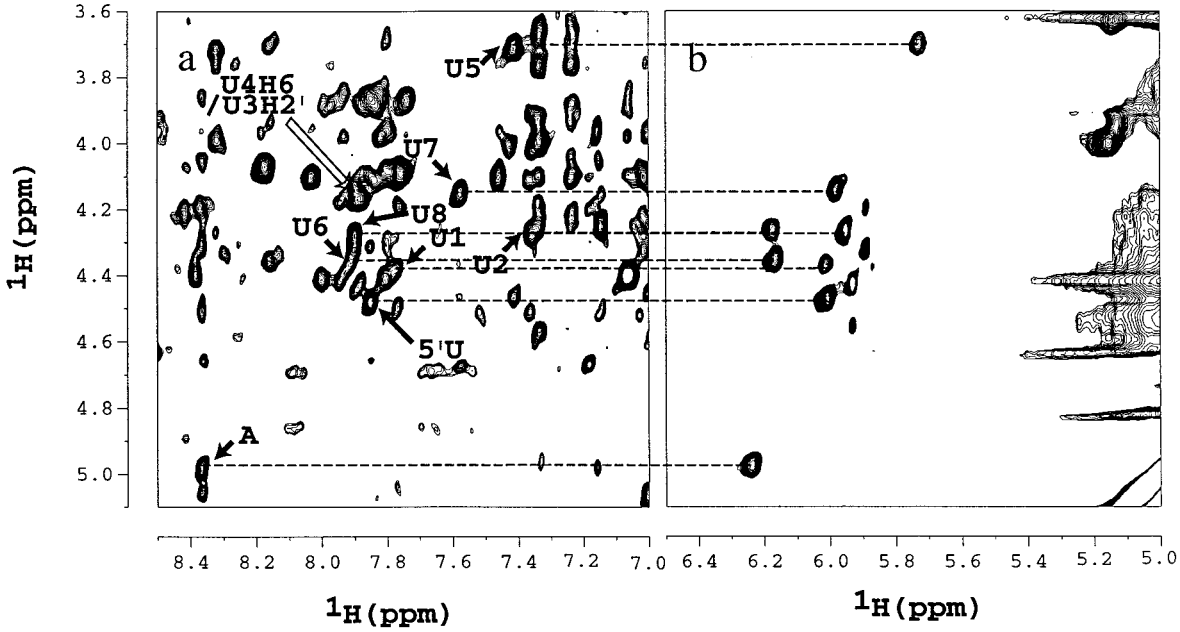

Figure 6. Regions of the NOESY (150-ms mixing time) (a) and TOCSY (b) spectra, connecting H2′ on the vertical axis with H8/H6 and H1′, respectively, on the horizontal axis of the complex of UAU_8 with the Sxl RBD1–RBD2 in ^2H_2O. The intra-nucleotide NOEs between H6/H8 and H2′ are indicated with filled arrows and the inter-nucleotide NOE with an open arrow.

C2′-endo ribose conformation

The ribose puckering conformation of RNA is mainly examined by the H1′-H2′ scalar coupling constant (Wijmenga et al., 1994; Kolk et al., 1998; Wijmenga and van Buuren, 1998). The relationship between the H1′-H2′ scalar coupling and the H1′-H2′ TOCSY coherence transfer was quantitatively analyzed by simulation (Wijmenga et al., 1994). According to that report, the intensity of the H1′-H2′ TOCSY cross peak in the C2′-*endo* conformation was more than 25 times stronger than that in the C3′-*endo* conformation at a 45-ms mixing time. Actually, in canonical A-form RNA, the ribose moieties are in the C3′-*endo* conformation and the H1′-H2′ scalar coupling constant is too small (< 2 Hz) to exhibit a cross peak in the TOCSY spectrum. In contrast, when the ribose moiety takes the C2′-*endo* conformation, considerable transfer occurs from H1′ to H2′, and the H1′-H2′ TOCSY cross peak was observed at a 45-ms mixing time (Wijmenga et al., 1994; Kolk et al., 1998). Therefore, a strong H1′-H2′ cross peak in the TOCSY spectrum indicates that the ribose moiety is predominantly in the unusual C2′-*endo* conformation with a much larger H1′-H2′ scalar coupling constant (ca. 10 Hz). In the case of UAU_8 complexed with the Sxl RBD1–RBD2, we observed eight strong H1′-H2′ cross peaks in the TOCSY spectrum (Figure 6b). The residues that showed strong cross peaks in the complex were 5′-U, A, U1, U2, U5, U6, U7, and U8 of the RNA. Since the H5-H6 scalar coupling constant is nearly 8 Hz, we compared the intensity of the H1′-H2′ TOCSY cross peak with that of the H5-H6 TOCSY cross peak of the same residue. Except for U5, the relative intensities were in the range of 0.6–0.8, which showed that the riboses of these residues were predominantly in the C2′-*endo* conformation (Wijmenga et al., 1994; Kolk et al., 1998). In the case of U5, the intensity of the H1′-H2′ TOCSY cross peak could not easily be compared with that of the H5-H6 TOCSY cross peak due to the difference of the line width of the resonance. Thus, we compared the intensity of the H1′-H2′ TOCSY cross peak with that of the H1′-H1′ TOCSY diagonal peak of the U5 residue. The relative intensity was over 1.0, which showed that the ribose of this residue was also in the C2′-*endo* conformation (Wijmenga et al., 1994). Therefore, these results indicated that the ribose moieties of the 5′-U, A, U1, U2, U5, U6, U7, and U8 of the RNA in the complex are in the C2′-*endo* conformation. These eight nucleotide residues with strong H1′-H2′ TOCSY cross peaks also showed strong intra-residue H6/H8-H2′ NOE cross peaks at a mixing time of 150 ms (Figure 6a). The

distances between H6/H8 and H2′ are dependent on both the χ torsion angle and the sugar puckering (Wijmenga and van Buuren, 1998). In the C2′-*endo* conformation, the absolute value of the χ torsion angle (C2-N1-C1′-O4′) is smaller than that in the C3′-*endo* conformation, and the H6/H8-H2′ distance is much shorter than that in the C3′-*endo* conformation. Thus, the unusually strong intra-residue H6/H8-H2′ NOEs are one of the characteristics of the C2′-*endo* conformation, together with the evidence showing the large coupling constant between H1′-H2′ (Wijmenga et al., 1994). Furthermore, these C2′-*endo* residues did not show any inter-residue H6/H8(*i*)-H2′($i-1$) NOE cross peaks, which means that each of these bases is unstacked from the preceding base. In contrast, U3 and U4 were found to be in the C3′-*endo* conformation, because they showed no detectable H1′-H2′ cross peaks in the TOCSY spectrum. Usually, a ribose moiety in the C3′-*endo* conformation shows a weak intra-residue H6/H8-H2′ NOE, while the inter-residue H6/H8(*i*)-H2′($i-1$) NOE is very strong because of the base stacking. In fact, inter-residue H6/H8(*i*)-H2′($i-1$) NOEs were observed only between U3 and U4. In contrast, between U2 and U3 and between U4 and U5, the bases seem to be unstacked, as no inter-residue NOEs were observed. In addition, another inter-residue NOE was observed between H5(U3) and H5(U4) (data not shown). This is also consistent with our consideration that these two bases, U3 and U4, have a stacking interaction.

In our previous crystallographic study on GU_2GU_8 complexed with the Sxl RBD1–RBD2 at 2.6-Å resolution (Handa et al., 1999), the ribose puckering conformations of GU_2GU_8 were analyzed by a common method, based on the distances between the 5′- and 3′-phosphorus atoms of 5.9 Å and 7.0 Å for C2′-*endo* and C3′-*endo*, respectively, in the canonical ordered structure of RNA (Sänger, 1983). Thus, we tentatively indicated that the ribose puckering conformations of all of the protein-bound nucleotide residues, except for that corresponding to U4 of AU_8, are the C2′-*endo* form (Handa et al., 1999). On the other hand, in the present study, the ribose conformations of UAU_8 complexed with the Sxl RBD1–RBD2 were unambiguously elucidated, from the H1′-H2′ correlation cross peaks, to be the C3′-*endo* form for U3 in addition to U4, and the C2′-*endo* form for the other nucleotide residues. As the nucleotide chain conformation between the residues corresponding to U2 and U3 is largely different from that in the canonical ordered structure (Handa et al., 1999), it is possible that the phosphorus-phosphorus distance is not regularly related to the ribose puckering at the U3 residue. The bases of the U3- and U4-corresponding residues of GU_2GU_8 are exceptionally stacked with each other (Handa et al., 1999). In this context, the base-stacking ribonucleotide residues are usually required to be in the C3′-*endo* form (Varani et al., 1996). Thus, an analysis of the diffraction data at 1.8-Å resolution is in progress in order to discriminate unambiguously between the C3′-*endo* and C2′-*endo* conformations for the Sxl RBD1–RBD2·GU_2GU_8 complex.

The C2′-*endo* form is rarely found within 'structured' RNAs with intensive intramolecular base pairing and stacking. In contrast, most of the nucleotide residues of the single-stranded uridine-rich RNAs bound with the Sxl RBD1–RBD2 are in the C2′-*endo* form, both in solution (the present study) and in the crystal (Handa et al., 1999). Similarly, in the recently reported structure of a poly(A) RNA bound with a poly(A) binding protein (PABP) fragment, which has two of the four RBDs (Deo et al., 1999), half of the nine adenosine residues were in the C2′-*endo* conformation with no base pairing hydrogen bond. In contrast, in the U1A·hairpin RNA, U1A·internal-loop RNA, and U2B″·U2A′·hairpin RNA complexes, only a few ribose moieties are in the C2′-*endo* conformation. In all of these base-paired RNA complexes, the bases of the residues in the C2′-*endo* form are stacked with the aromatic side chain at the second position of the RNP2 consensus motif (Oubridge et al., 1994; Allain et al., 1996; Price et al., 1998). The unusual feature that most of the protein-bound nucleotide residues are in the C2′-*endo* form may be characteristic of single-stranded RNAs with neither intramolecular nor intermolecular base pairing, and with extensive unstacking between the bases. The tandem arrangement of two (or more) RBDs may be important for the sequence-specific recognition of the single-stranded RNAs. By contrast, in the recently reported structure of the *trp* RNA-binding attenuation protein (TRAP) complexed with a single-stranded RNA (Antson et al., 1999), the nucleotide residues bound on the β-sheet are all in the C3′-*endo* conformation.

Conclusions

The H5-H6 proton resonance assignments of the polyuridine tract of the single-stranded RNA complexed with the Sxl RBD1–RBD2 were successfully achieved by site-specific [5-^{2}H]uridine substitutions.

Based on the unambiguous assignments of the proton resonances of the base moieties, we could analyze the interactions of the 5′-terminal region of the target RNAs with the protein, and the ribose conformations of all of the nucleotide residues in the protein-bound state. As compared with uniform ^{13}C-labeling of the RNA, the present method is more efficient and less expensive for the resonance assignments. These results demonstrate that this method of site-specific [5-^{2}H]uridine substitution is powerful for NMR analyses of single-stranded RNAs bound with multi-RBD proteins.

Acknowledgements

This work was supported in part by the ‘Research for the Future’ Program (JSPS-RFTF97L00503) from the Japan Society for the Promotion of Science. I.K. was supported by JSPS postdoctoral fellowships.

References

Allain, F.H.-T., Gubser, C.C., Howe, P.W.A., Nagai, K., Neuhaus, D. and Varani, G. (1996) *Nature*, **380**, 646–650.

Antson, A.A., Dodson, E.J., Dodson, G., Greaves, R.B., Chen, X.-P. and Collnick, P. (1999) *Nature*, **401**, 235–242.

Bax, A., Ikura, M., Kay, L.E., Torchia, D.A. and Tschudin, R. (1990) *J. Magn. Reson.*, **86**, 304–318.

Boggs, R.T., Gregor, P., Idriss, S., Belote, J.M. and McKeown, M. (1987) *Cell*, **50**, 739–747.

Burd, C.G. and Dreyfuss, G. (1994) *Science*, **265**, 615–621.

Deo, R.C., Bonanno, J.B., Sonenberg, N. and Burley, S.K. (1999) *Cell*, **98**, 835–845.

Ding, J., Hayashi, M.K., Zhang, Y., Manche, L., Krainer, A.R. and Xu, R.M. (1999) *Genes Dev.*, **13**, 1102–1115.

Földesi, A., Yamakage, S.-I., Nilsson, F.P.R., Maltseva, T.V. and Chattopadhyaya, J. (1996) *Nucleic Acids Res.*, **24**, 1187–1194.

Gubser, C.C. and Varani, G. (1996) *Biochemistry*, **35**, 2253–2267.

Hakimelahi, G.H., Proba, Z.A. and Oglivie, K.K. (1981) *Tetrahedron Lett.*, **22**, 5243–5246.

Handa, N., Nureki, O., Kurimoto, K., Kim, I., Sakamoto, H., Shimura, Y., Muto, Y. and Yokoyama, S. (1999) *Nature*, **398**, 579–585.

Howe, P.W.A., Allain, F.H.-T., Varani, G. and Neuhaus, D. (1998) *J. Biomol. NMR*, **11**, 59–84.

Inoue, K., Hoshijima, K., Sakamoto, H. and Shimura, Y. (1990) *Nature*, **344**, 461–463.

Inoue, M., Muto, Y., Sakamoto, H., Kigawa, T., Takio, K., Shimura, Y. and Yokoyama, S. (1997) *J. Mol. Biol.*, **272**, 82–94.

Kanaar, R., Lee, A.L., Rudner, D.Z., Wemmer, D.Z. and Rio, D.C. (1995) *EMBO J.*, **14**, 4530–4539.

Kim, I., Muto, Y., Inoue, M., Watanabe, S., Kitamura, A., Yokoyama, S., Hosono, K., Takaku, H., Ono, A., Kainosho, M., Sakamoto, H. and Shimura, Y. (1997) *Nucleic Acids Res.*, **25**, 1565–1569.

Kim, I., Watanabe, S., Muto, Y., Hosono, K., Takai, K., Takaku, H., Kawai, G., Watanabe, K. and Yokoyama, S. (1995) *Nucleic Acids Symp. Ser.*, **34**, 123–124.

Kolk, M.H., Wijmenga, S.S., Heus, H.A. and Hilbers, C.W. (1998) *J. Biomol. NMR*, **12**, 423–433.

Lee, A.L., Volkman, B.F., Robertson, S.A., Rudner, D.Z., Barbash, D.A., Cline, T.W., Kanaar, R., Rio, D.C. and Wemmer, D.E. (1997) *Biochemistry*, **36**, 14306–14317.

Mao, H. and Williamson, J.R. (1999) *Nucleic Acids Res.*, **27**, 4059–4070.

Oubridge, C., Ito, N., Evans, P.R., Teo, C.-H. and Nagai, K. (1994) *Nature*, **372**, 432–438.

Price, S.R., Ito, N., Oubridge, C., Avis, J.M. and Nagai, K. (1995) *J. Mol. Biol.*, **249**, 398–408.

Price, S.R., Evans, P.R. and Nagai, K. (1998) *Nature*, **394**, 645–650.

Puglisi, J.D. and Wyatt, J.R. (1995) *Methods Enzymol.*, **261**, 363–369.

Sakamoto, H., Inoue, K., Higuchi, I., Ono, Y. and Shimura, Y. (1992) *Nucleic Acids Res.*, **20**, 5533–5540.

Sakashita, E. and Sakamoto, H. (1994) *Nucleic Acids Res.*, **22**, 4082–4086.

Sänger, W. (1983) *Principles of Nucleic Acid Structure*, Springer Verlag, Berlin.

Singh, R., Valcárcel, J. and Green, M.R. (1995) *Science*, **268**, 1173–1176.

Sosnowski, B.A., Belote, J.M. and McKeown, M. (1989) *Cell*, **58**, 449–459.

Varani, G. and Nagai, K. (1998) *Annu. Rev. Biophys. Biomol. Struct.*, **27**, 407–445.

Varani, G., Aboul-ela, F. and Allain, F.H.-T. (1996) *Prog. NMR Spectrosc.*, **29**, 51–127.

Wataya, Y. and Hayatsu, H. (1972) *J. Am. Chem. Soc.*, **94**, 8927–8928.

Wijmenga, S.S., Heus, H.A., Werten, B., van der Marel, G.A., van Boom, J.H. and Hilbers, C.W. (1994) *J. Magn. Reson.*, **B103**, 134–141.

Wijmenga, S.S. and van Buuren, B.N.M. (1998) *Prog. NMR Spectrosc.*, **32**, 287–387.

Zawadzki, V. and Gross, H.J. (1991) *Nucleic Acids Res.*, **19**, 1948.

Zhou, S., Yang, Y., Scott, M.J., Pannuti, A., Fehr, K.C., Eisen, A., Koonin, E.V., Fouts, D.L., Wrightsman, R., Manning, J.E. and Lucchesi, J.C. (1995) *EMBO J.*, **14**, 2884–2895.